JuniKhyat
ISSN: 2278-4632
(UGC Care Group I Listed Journal)
Vol-13 Issue-02 July 2023

Antenna with Frequency and Pattern Re configurability for Future Wireless Networks

A B S R Manohar, K. Murali Babu, Jaya Kumar K

Assoc. Professor and HOD[1], Asst. Professor[2,3]

Dept. of Electronics and Communication Engineeering,

Bhimavaram Institute of Engineering and Technology, Bhimavaram, Andhra Predesh, India.

E.mail id: manu.abd@gmail.com, k.murali1289@gmail.com, kjkumar123@gmail.com

Abstract: In this paper, we offer a miniature, printed antenna that can change its frequency and its radiation pattern. This paper proposes an antenna with three individual toggles. Antenna band selection is handled by the lumped Switch 1. The antenna's beam direction is controlled by the second and third switches. With Switch 1 engaged, the proposed antenna works across the 2.5-4.2 GHz and 6.2-7.4 GHz bands, at 3.1 GHz and 6.8 GHz, respectively. When Switch 1 is off, the antenna can only pick up signals between 2.5 and 4.2 GHz on the 3.1 GHz frequency. The antenna's beam may be tailored by toggling Switches 2 and 3 on and off. The states of Switches 2 and 3 may be combined to create a wide variety of beams. In each of the four scenarios, the increase is larger than 3.7 dBi.

Keywords: pattern reconfigurable; patch antenna; s-parameters; frequency reconfigurable

1. Introduction

2. Because of their potential uses in a wide range of wireless communication systems, reconfigurable antennas have attracted a lot of attention as communication technology has advanced. You may tailor their characteristics to get the frequency range, emission pattern, and polarization you need. The negative effects of co-channel interference and jamming can be mitigated by using a tunable antenna instead of a wide band antenna due to the former's smaller size, comparable radiation patterns across all multiple frequency bands, productive utilization of electromagnetic range, and frequency discernment [1,2]. Tuning a single attribute of an antenna has been the primary emphasis of previous research, rather than a number of qualities. Frequency reconfigurability has been achieved by inserting microfluidic controlled polypropylene tubes between the primary radiators and the ground plane [3]. The bandwidth of the antenna may be changed from narrow to broad by using a pin diode, and the bandwidth can be constantly changed using a varactor diode. narrow band resonance frequency [4] that makes it competitive for use in cognitive radio. In [5], we saw a printed monopole antenna for WLAN/WiMAX that could be tuned to many frequencies using a PIN diode. Using voltage-controlled varactor diodes, a large frequency tuning range was obtained in a probe-feed patch antenna [6]. In [7], a printed antenna with a hooked form and stub load that may change frequencies for different uses is introduced. In [8,9], frequency tuning was accomplished with the use of lumped switches. PIN and varactor diodes were used to provide frequency tuning in [10]. In [11], researchers looked at how to tune the frequency of a Vivaldi antenna. Beams may be redirected with the use of high-impedance surfaces [12], loops with diodes [13], numerous lumped switches [14], and multiple diodes in an asymmetrical fashion [15]. In [16], a metamaterial-based, dual-polarized antenna that operates at a variety of frequencies is described. In [17], a dual-band antenna using varactor diodes for separately adjustable bands is shown.

Configurations where the frequency and pattern of the system may be modified separately are necessary due to the fast growth of communication networks. It is difficult to create a single antenna that can accommodate all of these different layouts. Some antennas with adjustable frequency and radiation pattern have been developed in recent years. In [18], the authors describe a PIN diode-based slot antenna with frequency and pattern reconfigurability. The antenna's four slits and two switches allow for pattern reconfigurability and the generation of various resonant bands. Neither the elevation nor the azimuth planes are fully covered by the antenna illustrated in [18]. The complexity of the system and the insertion losses are both increased by the usage of so many RF PIN diodes in the aforementioned antenna. In [19], frequency and pattern reconfigurability is achieved by the use of numerous pin diodes. Although the antenna performs well at each standard, its excessive bulk prevents it from being used in most cutting-edge forms of communication. By inserting PIN diodes into the annular slot, the main lobe and the null may be steered in the desired direction, as shown in [20]. Matching stubs are used to change the resonant frequency. In [21], frequency and pattern reconfigurability in the antenna are achieved by the use of liquid crystal technology. Slits coupled through PIN diodes to the primary radiating portion allow for frequency and pattern reconfigurability, as shown in [22]. Antenna of [22]'s design.

may only adjust the angle of emission by 90°, 180°, 270°. For both 1.9 G and 2.4 G frequencies, a flexible antenna is suggested.

in [23] with the ability to change frequencies and adjust beams. The antenna's complicated construction (more RF diodes) and big size make it unsuitable for today's wireless communication architecture. In [24], a beam-steering and frequency-shifting array antenna constructed from stub and varactor diodes is shown; nevertheless, the antenna's beam-shifting performance is limited (30 to +30) and its physical bulk is prohibitive. In [25], an array antenna built on High Impedance Structures (HISs) is said to have a high gain. The antenna's frequency and partial pattern may be changed (+/- 11° phase shift) with the use of four pin diodes. In [26], we see a frequency-switching antenna with three different beamwidths. To tune the resonant bands, a pair of PIN diodes is placed in a slot etched into the antenna's top face, and a second pair is added to the feeding network to facilitate beam shifting.

By demonstrating how to separately alter the system's frequency and pattern, this study offers the greatest method for accelerating the creation of communication system configurations. While two lumped switches (Switch 2 and Switch 3) are deployed inside the ground to generate pattern reconfigurability, the proposed antenna may operate in either single- or dual-frequency mode, depending on the state of the lumped switch (Switch 1).

3. Antenna’s Design Methodology

Figure 1 depicts the proposed antenna's configuration. The proposed antenna's patch and ground are printed on a FR-4 substrate that is 1.6 mm thicker and has a dielectric constant of 4.4. The dimensions of the suggested antenna are just 23 mm by 31 mm by 1.6 mm. The typical impedance of the 3 mm wide microstrip transmission line is 50. Table 1 provides the values for the different characteristics of the proposed antenna.

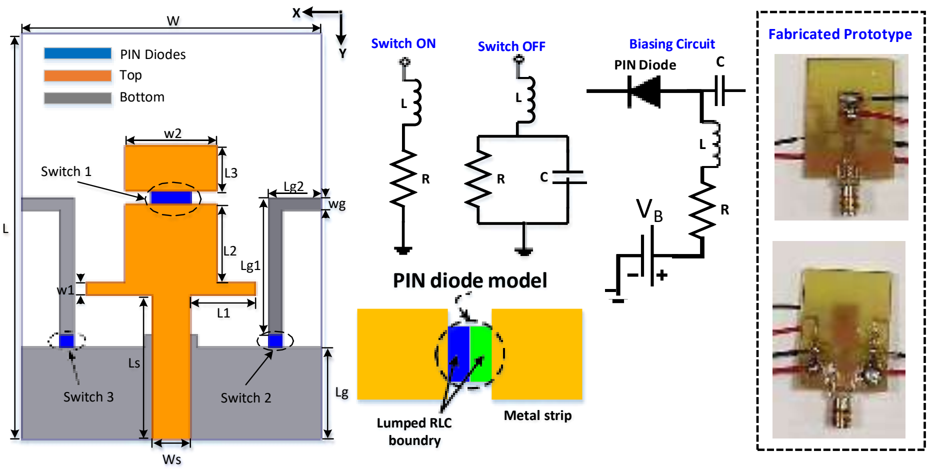

Figure 1. Proposed antenna diagram, biasing circuit for PIN diode and Fabricated antenna.

Table 1. Different Parameter and values of the antenna.

Parameter	Value (mm)	Parameter	Value (mm)	Parameter	Value (mm)
W	23	L1	5.05	Lg2	4
L	31	L2	6	Lg1	10.5
L3	3.5	W1	1	Wg	1
W2	7	Ws	3	Lg	7
Ls	9.5				

Equation (1) is used to calculate the length of the radiating element [27].

$$L_{f_r} = \frac{c}{4 f_r \sqrt{e_{eff}}} \quad (1)$$

$$e_{eff} \approx \frac{e_r + 1}{2} + \frac{e_r - 1}{2}\left(1 + 12\left(\frac{w}{h}\right)\right)^{-0.5} \quad (2)$$

For each of the preceding equations, "c" represents the speed of light in a vacuum, "g" represents the guided wavelength, "ee f f " represents the effective dielectric constant, and "w" and "h" represent the substrate's width and thickness, respectively. While (1) and (2) provide a monopole length of 11.91 mm, the optimal monopole length (L1 + L2) is 11.05 mm.

For each switching state, the antenna's reflection coefficient response is observed by connecting a unique set of stubs to the ground plane. In example 1, the antenna has an excellent impedance match at 3.5 GHz and 6.7 GHz when connected to the ground through an I-shaped stub (Figure 2a). In cases 2 and 3, the antenna has a resonant frequency of 3.9 GHz and 6.7 GHz, respectively. In example 4, the antenna only resonates at higher frequencies due to an impedance mismatch at lower frequencies. Step two involves loading the H-shaped stub onto the ground plane, as seen in Figure 2b. When switch 1 is activated and all other switches are off, the antenna resonates at 3.5 GHz and 7.3 GHz. In cases 2 and 3, the antenna resonant frequency is 3.5 GHz, whereas in example 1 it is 7.3 GHz. In example 4, the impedance matches rather well at higher frequencies but mismatches at lower ones. Figure 2c shows the results for all four scenarios when an L-shaped stub is put into the ground plane. The antenna's performance as measured by the reflection coefficient is excellent across the board.

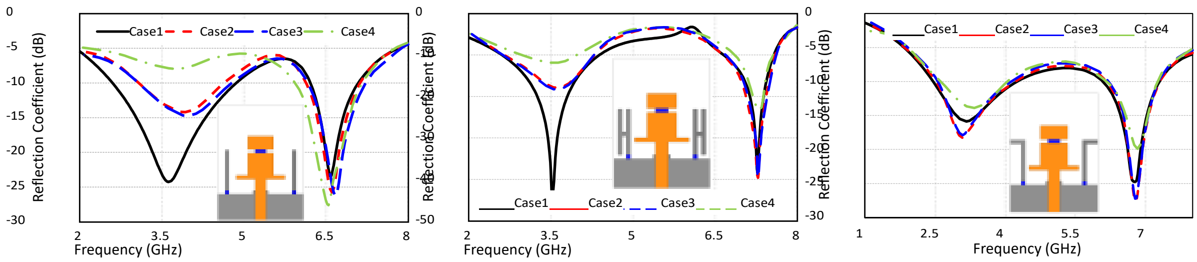

(**a**) (**b**) (**c**)

Figure 2. Reflection coefficient analysis for all cases with (**a**) I-shaped stub, (**b**) H-shaped stub, (**c**) L-shaped stub.

3.1. *Switching Techniques*

In the RF spectrum, a PIN diode often acts like a variable resistor, although its ON and OFF states involve more complicated circuitry. In both the ON and OFF states of the PIN diode, an inductor (L) and a resistor (R) make up the equivalent circuit. When the inductor and resistor (R) are connected in series, a forward bias is created for the diode. When the switch is turned off, a resistor (R) and capacitor (C) are connected in parallel with the inductor. Both the ON and OFF states of the PIN diode are analyzed as RL and RLC circuits [28]. In an RL circuit, current may flow between the radiating components because R has a low enough value. In an RLC circuit, the greater value of RC prevents current from passing between the radiating components. As a result, we simulated our PIN diode as a simple RL circuit for the purpose of clarity. There is no change to the inductor's (L) value. When the diode is active, the value of its associated resistor (R) is maintained low at 1, but when it is inactive, it is set high at 5 M. The circuitry receives a biasing voltage (VB) of 3 V in the ON state and 0 V in the OFF state.

3.2. *Antenna's Parametric Analysis*

The suggested antenna was developed using the High Frequency Structure Simulator (HFSS 13.0). Figure 3 shows the reflection coefficient (S11) of the planned antenna in the ON and OFF modes of switch 1. In the OFF position of Switch 1, as shown in Figure 3, the proposed antenna operates in a single frequency range. As can be seen in Figure 3, switching to the ON position of Switch 1 results in dual band antenna performance.

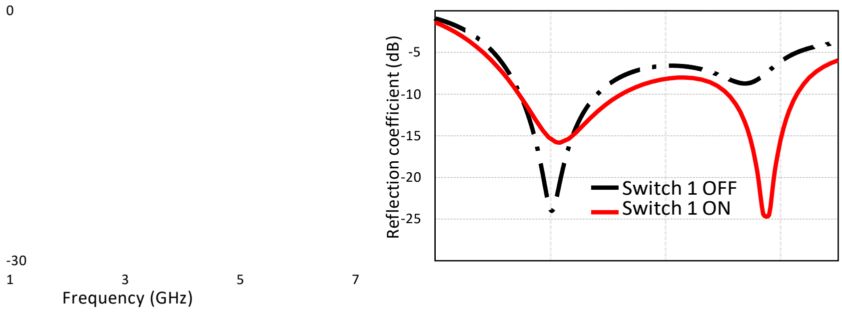

Figure 3. Reflection coefficient of the proposed antenna at ON and OFF switch.

The performance of the proposed antenna is analyzed as a function of a number of factors, or "parameter scans." w1 and L2 are used to evaluate the proposed antenna's performance. The band about 6.8 GHz is quite sensitive to the value of w1, as seen by the graph of changing this parameter. The 6.8 GHz band's resonance frequency is very sensitive to the value of the parameter w1. The first resonant band is little affected by a change in the value of the parameter w1, whereas the second band's resonant frequency changes toward the lower frequency. Parametric analysis supports the conclusion that the second

The parameter w1 determines the width of the resonant band. The suggested antenna's S11 at different frequencies and w1 values is shown in Figure 4a, which was generated using simulation.

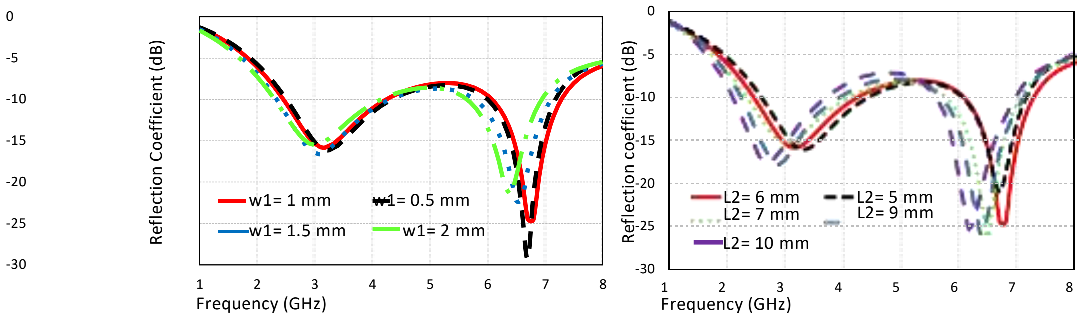

(a) (b)

Figure 4. Reflection coefficient against frequencies for varied parameter (**a**) $w1$ (**b**) $L2$.

4. For various values of the parameter L2, the simulated S11 of the proposed antenna is shown as a function of frequency in Figure 4b. The image makes it quite evident that the parameter L2 may effectively move both bands. As L2 is increased, a lower frequency is reached by both bands. It is evident from [27] that the frequency decreases as the length of the monopole increases. As the length of the radiating element grows (1), the operational frequency drops.

5. Results and Discussions

The top and bottom of the manufactured antenna are shown in Figure 1. The manufactured antenna makes use of an MPP4203 (Microsemi) low-capacitance PIN diode. There is a perfect separation between the DC route and the feeding path. The RF choke (RFC) can block RF and pass DC, whereas capacitors may do the opposite. A 125 nH inductor and a 470 pF capacitor are used to create the antenna. The gain and reflection coefficient of the prototype are evaluated using an Agilent Vector Network Analyzer (VNA). The SOLT (short-open-load-through) method is used for the VNA's calibration. The reflection coefficient is measured by connecting the finished prototype to the VNA after the VNA has been calibrated. For far field pattern measurements, a 6dB log periodic antenna is deployed 8 m from the planned antenna. The finished antenna is mounted on a turntable and rotated by motor in 10° increments along both principal axes.
Figure 5 depicts the proposed antenna's resonance frequency of 3.1 GHz when the lumped switch (Switch 1) is turned off, with a 10 dB bandwidth of 1.7 GHz. When the combined switch is activated (Switch 1), the antenna operates in a dual-band mode. Resonant frequencies for the antenna are 3.1 GHz and

When the lumped switch of the proposed antenna is activated, its operating frequency range expands to 6.8 GHz, spanning 10 dB bandwidths of 1.7 GHz and 1.2 GHz, respectively.

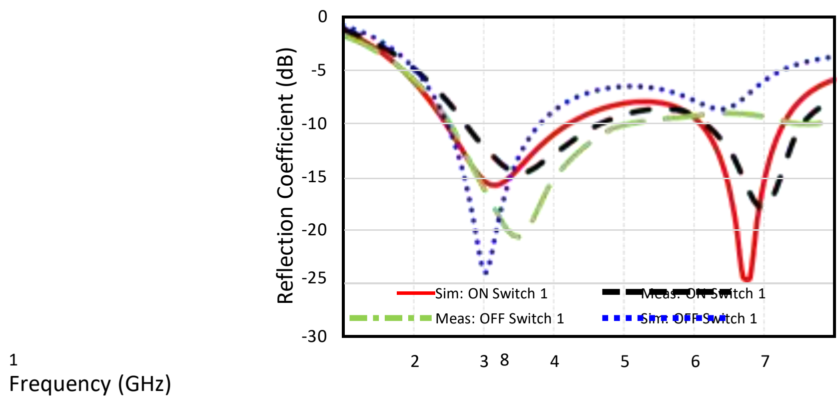

Figure 5. Simulated and measured reflection coefficient of the proposed antenna.

Reflection coefficient (S11) measurements for the ON and OFF states of the switch (Switch 1) are compared in Figure 5. The predicted and observed outcomes are consistent with one another. The three lumped switches in the manufactured antenna, the losses in the SMA connection, and the cable losses all contribute to the little discrepancy in the S11 curves.

Surface current distributions at 3.1 GHz and 6.8 GHz are shown in Figure 6 to further describe the proposed antenna's behavior. Figure 6 shows that at 3.1 GHz, the current density is greatest near the bottom of the radiator in comparison to the rest of the component. Resonance at 3.1 GHz may be traced down to the lower area, as seen in Figure 6. At 6.8 GHz, the proposed antenna's surface current density is larger at both the lower and upper sections of the antenna, suggesting that both the lower and top parts of the antenna contribute to the antenna's 6.8 GHz resonance. Figure 7 shows the antenna's simulated gain and efficiency in all switching scenarios.

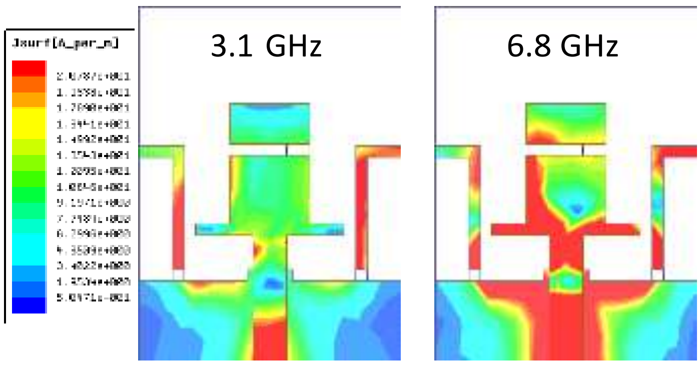

Figure 6. Surface current density of the proposed antenna at ON switch condition.

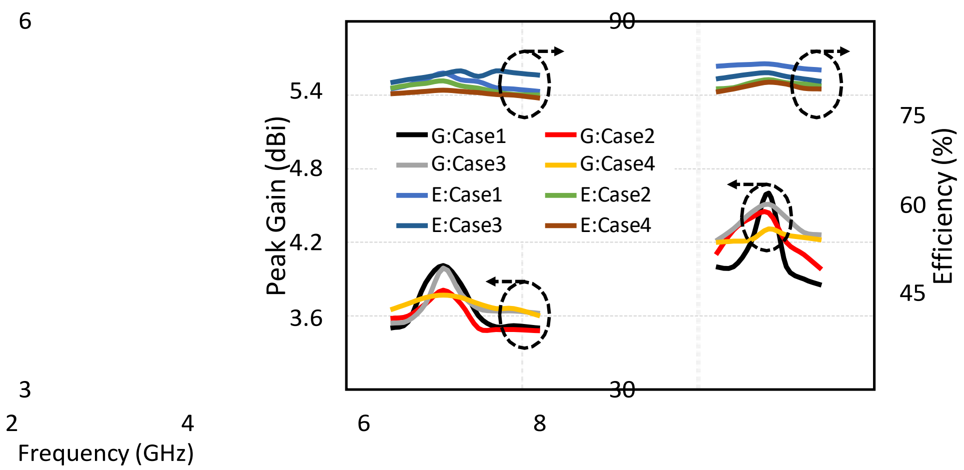

Figure 7. Simulated peak gains and efficiencies for all switching cases (G = Peak gain and E = efficiency).

Radiation patterns in cases 1, 2, 3, and 4 are shown in Figures 8 through 11. Phi = 0 and Phi = 90 radiation patterns are modeled and evaluated. Radiation patterns at 3.1 and 6.8 GHz for the proposed antenna have been modeled and compared to measurements in all circumstances. Antenna impedance and radiation characteristics are affected by the ground plane's size and structure because of the time-varying current on the ground plane. The addition of a ground-based L-shaped stub has a little effect on impedance but a dramatic effect on antenna radiation. Different beam tilting phenomena result from the unique current distribution seen in each switching scenario (Figure 12).

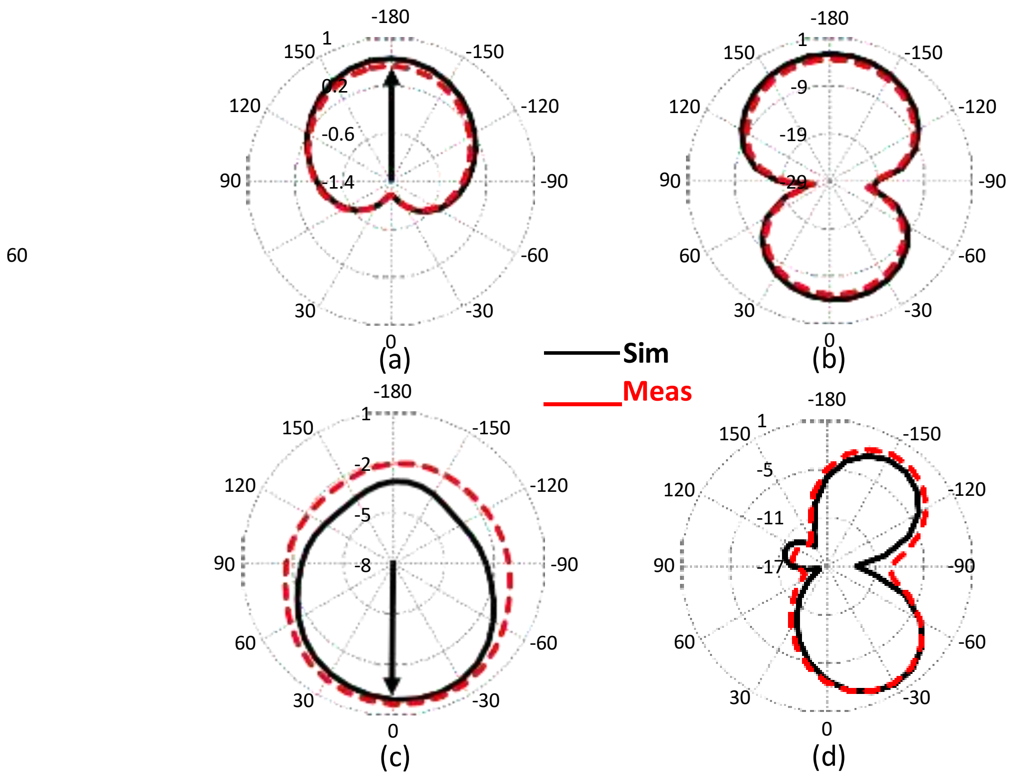

Figure 8. Case 1: (**a**) Phi = 0° at 3.1 GHz (**b**) Phi = 90° at 3.1 GHz (**c**) Phi = 0° at 6.8 GHz (**d**) Phi = 90° at 6.8 GHz.

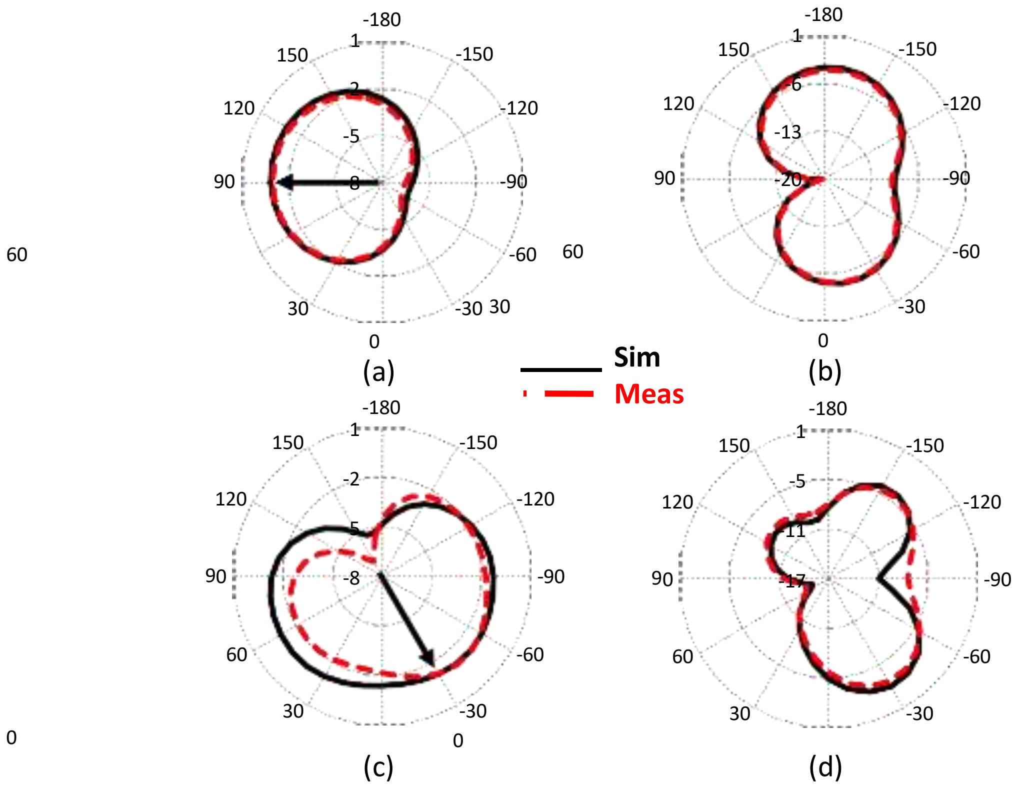

Figure 9. Case 2: (**a**) Phi = 0° at 3.1 GHz (**b**) Phi = 90° at 3.1 GHz (**c**) Phi = 0° at 6.8 GHz (**d**) Phi = 90° at 6.8 GHz.

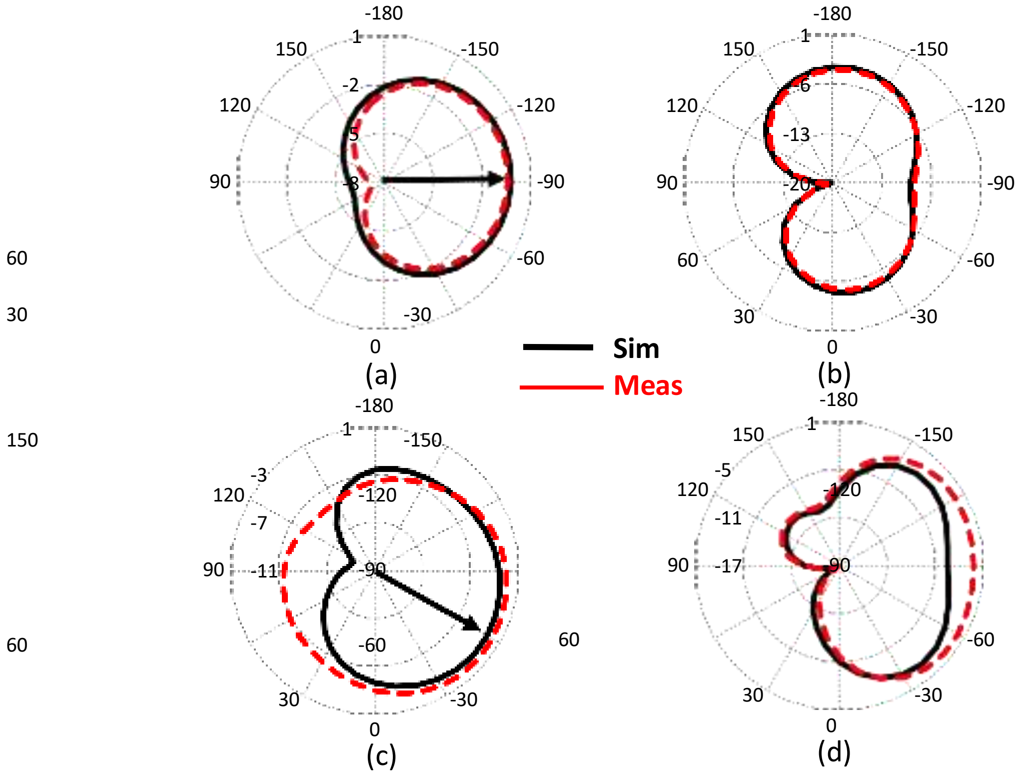

Figure 10. Case 3: (**a**) Phi = 0° at 3.1 GHz (**b**) Phi = 90° at 3.1 GHz (**c**) Phi = 0° at 6.8 GHz (**d**) Phi = 90° at 6.8 GHz.

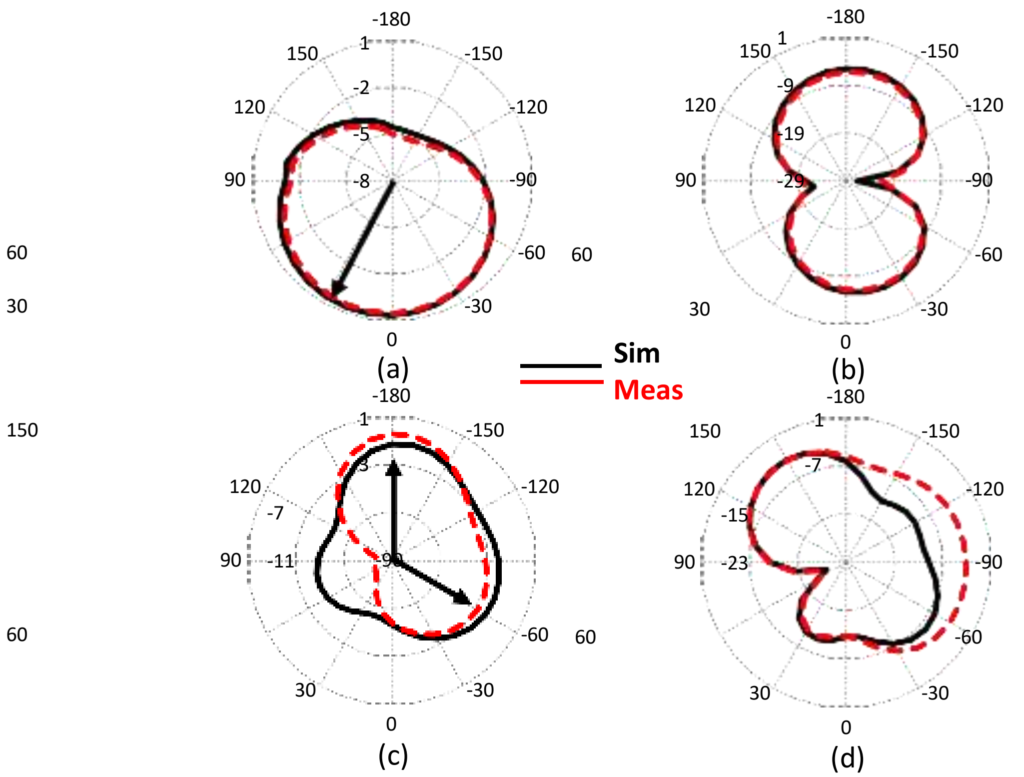

Figure 11. Case 4: (**a**) Phi = 0° at 3.1 GHz (**b**) Phi = 90° at 3.1 GHz (**c**) Phi = 0° at 6.8 GHz (**d**) Phi = 90° at 6.8 GHz.

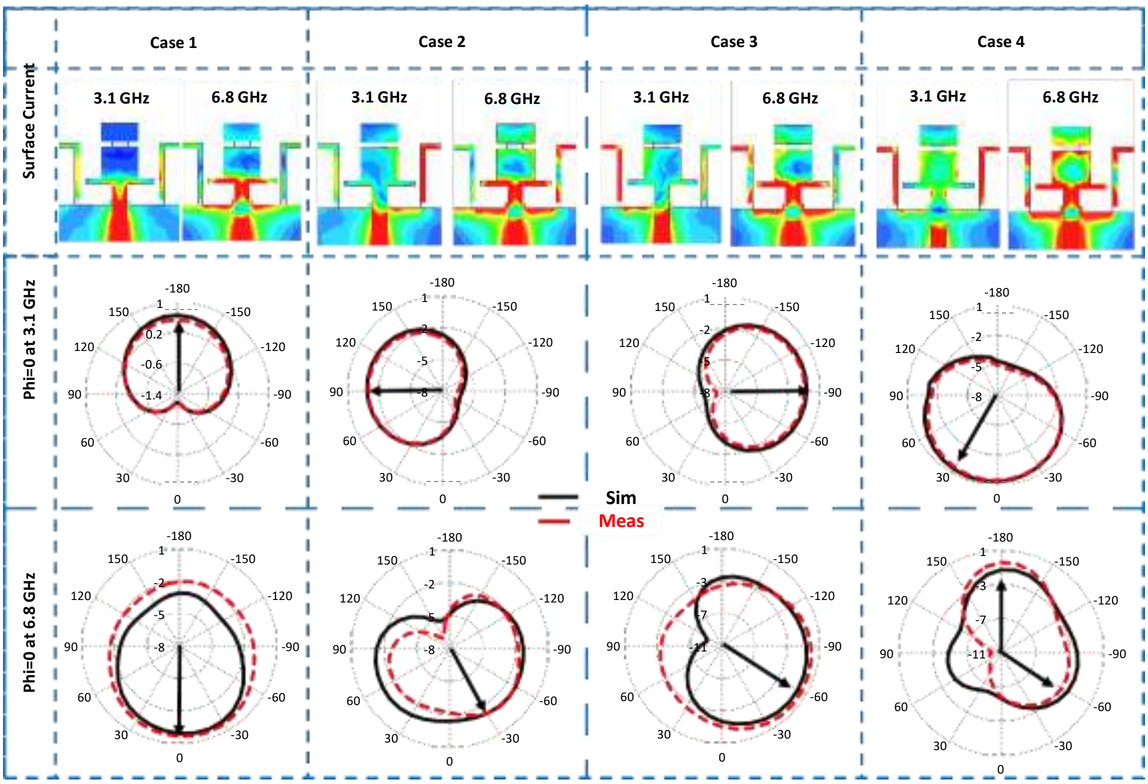

Case 1: *sw1=ON, sw2=OFF, sw3=OFF,* **Case 2:** *sw1=ON, sw2=ON, sw3=OFF,* **Case 3:** *sw1=ON, sw2=OFF, sw3=ON,* **Case 4:** *sw1=ON, sw2=ON, sw3=ON*

Figure 12. Summary of the beam switching using switch 2 and switch 3.

Case 1's radiation pattern, seen in Figure 8, occurs when Switch 1 is activated while the other switches are turned off. Figure 8 shows that the major lobe at Phi = 0 is pointed in the direction of 180, whereas the main lobe at 3.1 GHz is quite small in comparison. A low backward lobe is seen at 6.8 GHz, with the primary lobe pointing in the direction of 0 in the Phi = 0 plane. The planned antenna radiates mostly as a "Figure of Eight" in the Phi = 90 plane at lower frequencies, although some distortion is seen at higher frequencies.

Radiation pattern for Case 2 with Switches 1 and 2 ON and Switch 3 OFF is seen in Figure 9. The current in this scenario follows the ground plane's L-shaped connection with the stub. This is seen in Figure 12. Since most of the current is concentrated on the right side of the L, the beam is boosted in one direction (by 90 degrees at 3.1 GHz and by 30 degrees at 6.8 GHz) while attenuated in the other. Figure 9 shows that the proposed antenna's primary lobe is aimed at 90 degrees for Phi = 0 degrees at 3.1 GHz, and that it is aimed at 30 degrees at 6.8 GHz. The planned antenna emits most of its energy in the form of a distorted "Figure of Eight" on the Phi = 90° plane at low frequencies, but at high frequencies the distortion is much more pronounced.

Radiation pattern for Case 3 with Switches 1 and 3 ON and Switch 2 OFF is seen in Figure 10. The L-shaped stub on the left side of the ground plane (Figure 12) acts as a director to tilt the beam to the right by 90 degrees at 3.1 GHz and 60 degrees at 6.8 GHz. Figure 10 shows that the suggested antenna's primary lobe is pointed in the direction of 270 for Phi = 0 at 3.1 GHz and in the direction of 60 at 6.8 GHz.

Case 4's radiation pattern with all three switches engaged is seen in Figure 11. Because the ground plane current is focused on both L-shaped stubs, the power in the opposite direction is suppressed (the beam is directed at 30 degrees for 3.1 GHz and 60 degrees/180 degrees for 6.8 GHz). Figure 11 shows that the proposed antenna's primary lobe is aimed at 30 for Phi = 0 at 3.1 GHz, and that at 6.8 GHz, it is aimed at 60 and 180. The suggested antenna has a consistent radiation pattern across all four scenarios. The directed beams also have acceptable front-to-back ratios (FBR).

The suggested antenna's pattern may be reconfigured by modifying the switching states, as shown in Table 2. In Table 3, we see how the antenna's simulated efficiency, measured efficiency, and measured gain differ across four distinct scenarios. Table 3 shows that the antenna has high theoretical and actual gain and adequate theoretical efficiency in four different scenarios. The suggested antenna is compared to others in the literature in Table 4. The suggested antenna is unusual because to its ability to effectively change its frequency and beam direction while maintaining its basic design. It is worth noting that the suggested antenna is more compact than others described in the literature. In addition, the suggested antenna utilizes a minimal number of switches, which both minimizes the complexity of the design and the losses incurred by the switches. The antenna provided here offers a better peak gain and a broader bandwidth than those currently available.

Table 2. Summary of the state of switches and corresponding main lobe direction.

Case	Switch 1	Switch 2	Switch 3	Main Lobe Direction at Phi = 0° for 3.1 GHz	Main Lobe Direction at Phi = 0° for 6.8 GHz
1	ON	OFF	OFF	180°	0°
2	ON	ON	OFF	90°	−30°
3	ON	OFF	ON	−90°	−60°
4	ON	ON	ON	30°	−60° and 180°

Table 3. Summary of the different cases and its corresponding gains and efficiencies at both bands.

Case	Gain (dBi)		Efficiency (%)	Gain (dBi)		Efficiency (%)
	Sim (3.1 GHz)	Meas (3.1 GHz)		Sim (6.8 GHz)	Meas (6.8 GHz)	
1	4.01	3.93	81.6	4.60	4.58	83.1
2	3.81	3.78	80.3	4.44	4.35	80.5
3	3.99	3.89	81.4	4.51	4.46	81.6
4	3.77	3.70	78.8	4.31	4.21	80.1

Table 4. Performance comparison with previously published work.

Ref.	Size (mm^2)	Reconfiguration	Actuators	Bandwidth (MHz)	Peak Gain (dBi)
[18]	130 × 160	Frequency and Pattern	11 PIN diodes	200/150/150	5.6/4.6/3.3
[19]	80 × 45.8	Frequency and Pattern	5 PIN diodes	580/290	2.1/4.8
[20]	50 × 50	Frequency and Pattern	2 PIN diodes	100/70	4/5.6
[22]	50 × 50	Frequency and Pattern	4 PIN diodes	180/200/180/200	4/3.8/4.4/5
[23]	42 × 44	Frequency and Pattern	8 PIN diodes	160/220	NG
[24]	160.9 × 151.5	Frequency and Pattern	2 Varactor diodes	230	9
[25]	70 × 70	Frequency and Pattern	4 PIN diodes	NG	0.521/7.833
[26]	40 × 30	Frequency and Pattern	4 PIN diodes	400/500	2.24–2.76
This Work	23 × 31	Frequency and Pattern	3 PIN diodes	1700/1200	4.01/4.60

6. Conclusions

This study presents the design and experimental validation of a small printed antenna with the capabilities of frequency shifting and pattern reconfigurability. The suggested antenna's performance varies depending on whether Switch 1 is on or off. Switch 1 determines which of two possible frequencies may be used by the proposed antenna. Switch 1's OFF position allows the antenna to transmit at 3.1 GHz. Depending on the setting of Switch 1, the antenna may provide usable gains of 4.01 dBi (in the UWB health monitoring spectrum for dogs) and 4.6 dBi (in the indoor UWB band). Modifying the ground plane's Switch 2 and Switch 3's states yields pattern reconfigurability. By switching the states of Switch 2 and Switch 3, we can generate four distinct beam orientations while still retaining high gain and efficiency.

References

1. Authors: 1, Augustin, G.; 2, Aanandan, C.; 3, Mohanan, P.; 4, Vasudevan, K. Microstrip antenna with a switchable load of two slots, each operating at a different frequency. Microwave Optical Technology Letters 2005, 44, 374–376.

2. 2. Ojaroudi Recent Developments of Reconfigurable Antennas for Present and Future Wireless Communication Systems. Parchin, N.; Jahanbakhsh Basherlou, H.; Al-Yasir, Y.I.; Abd-Alhameed, R.A.; Abdulkhaleq, A.M.; Noras, J.M. There are just 128 pages in the 2019 edition of Electronics. [CrossRef]

3. Microfluidically frequency-reconfigurable microstrip patch antenna and array. Tang, H., and Chen, J.X.

4. 2017 (2017), 5 (20470-20476) IEEE Access. [CrossRef]

5. Compact, Frequency-Reconfigurable Filtenna with Sharply Defined Wideband and Continuously Tunable Narrowband States. 4. Tang, M.C.; Wen, Z.; Wang, H.; Li, M.; Ziolkowski, R.W. Antennas Propagation, IEEE Transactions on, 2017, 65:5026-5034. [CrossRef]

6. Five Abdulraheem authors: Y.I.; Oguntala; G.A.; A.S.; H.J.; Mohammed; R.A.; Ali; R.A.; Abd-Alhameed; J.M. Utilizing two PIN diodes, a small multiband antenna was designed for WLAN/WiMAX networks. 2017;11(11):1098-1105 in IET Microw. Antennas Propag. [CrossRef]

7. Rmili, H., Trabelsi, H., and Rouissi, I.F.M. Capacitive loading and a varactor diode were used in the development of a patch antenna with tunable frequency characteristics. Lisbon, Portugal, April 13–17, 2015; pp. 1–4; 9th European Conference on Antennas and Propagation (EuCAP) proceedings.

8. Seventh, Sharma, N., M. Yadav, and A. Kumar designed a frequency reconfigurable antenna that can operate on many frequencies simultaneously. Noida, India, February 2-3, 2017; pp. 275-279 in Proceedings of the 2017 Fourth International Conference on Signal Processing and Integrated Networks (SPIN).

9. The eight authors are: Iqbal, A.; Ullah, S.; Naeem, U.; Basir, A.; Ali, U. A small, frequency-tunable, modified-T-shape planar antenna was designed, built, and tested for use in handheld devices. 2017;12(12):1611-1618 J. Electr. Eng. & Technol.

10. A. Iqbal and O.A. Saraereh, 9. A Small Monopole Antenna that Can Change Frequencies for WLAN and Wi-Fi Use. 2017;68:79-84 in Progress in Electromagnetic Research.

11. Xiong, J.; Yu, Y.; He, S.; Li, H. This slot antenna may be tuned across a broad frequency range and is easily reconfigured.

12. 2010; 58:3725-3728 IEEE Trans. Antennas Propag. [CrossRef]

13. Eleven Hamid, M.R., P. Gardner, P. Hall, P.S. Ghanem, and F. The antenna is a re-configurable Vivaldi. Microwave Optics and Technology Letters. 52:787–787 (2010). [CrossRef]

14. A. Deo, P. Mehta, D. Mirshekar-Syahkal, and H. Nakano. A spiral antenna that may change its radiation pattern using a hybrid information system. IEEE Transactions on Antennas and Propagation Letters, Vol. 8, No. 1, Pages 196–199, 2009. [CrossRef]

15. Kang, W., S. Lee, and K. Kim. An antenna with a switchable beam pattern has been designed. Electronics Letters. 46(10):1536-1537, 2010. [CrossRef]

16. A pattern reconfigurable microstrip parasitic array. Zhang, S., G. Huff, J. Feng, and J. Bernhard. 2004, 52, 2773–2776, IEEE Trans. Antennas Propag. [CrossRef]

17. Cai, X., A. Wang, and W. Chen ranked 15th. An antenna in the form of a disc that can change its frequency and radiation pattern. Hangzhou, China; 20-22 April 2011; pp. 1–4; 2011 China-Japan Joint Microwave Conference Proceedings (CJMW).

18. Chen, X., and Zhao, Y. Double-Layer Metasurface-Based Dual-Band Polarization and Frequency-

Configurable Antenna. Electronic Communications (AEU-International), 95 (2018), 82–87. [CrossRef]

19. Hall, L.; Fumeaux, C.; Nguyen-Trong, N. An antenna capable of changing frequencies and patterns in two separate bands.

20. Microwave and Optical Technology Letters 59, 2710–2715 (2017). [CrossRef]

21. F. Majid; M.K.A. Rahim; M.R. Hamid; M.F. Ismail; F. Slot Antenna That Can Be Reconfigured for Different Frequencies and Patterns.

22. Antennas Propagation, IEEE Transactions on (2014), 62, 5339–5343. [CrossRef]

23. Frequency and Pattern Reconfigurable Antenna for Multi-Standard Wireless Applications. Li P.K., Shao Z.H., Wang Q., Cheng Y.J. 2015, 1a, D3st Group.

24. Twenty Nikolaou, S., B. Bairavasubramanian, C. Lugo, I. Carrasquillo, D.C. Thompson, G.E. Ponchak, J. Papapolymerou, M.M. Tentzeris, and M.M. An PIN diode-based annular slot antenna with pattern and frequency reconfigurability. 2006, 54:439-448 IEEE Trans. Antennas Propag. [CrossRef]

25. An Antenna Array That Can Change Its Frequency and Pattern Using Liquid Crystal Technology, by Zhao, Y., Huang, C., Qing, A., and Luo, X. 2017;9(1):1-7. IEEE Photonics Journal. [CrossRef]

26. 22, Selvam, Y.P., Kanagasabai, M., Alsath, M.G.N., Velan, S., Kingsly, S., Subbaraj, S., Rao, Y.V.R., Srinivasan, R., Varadhan, A.K., and Karuppiah, M. An Easily Adjustable Antenna for Frequency and Pattern that Takes Up Little Space. 2017;16(10):3047-3050 IEEE Antennas Wired Propagation Letters. [CrossRef]

27. An Antenna with Reconfigurable Frequency and Pattern for Wireless Systems, by Zhu, Wang, You, and Gao (No. 23). Progress in Electromagnetic Research, 76, 63–70 (2018).

28. Fumeaux, C.; Nguyen-Trong, N.; Zainarry, S.N.M. A Two-Element Array Antenna That Can Be Changed in Both Frequency and Pattern. 2018;17(12):617-620 IEEE Antennas Wired Propagation Letters. [CrossRef]

29. R. Dewan; M.K. Abd Rahim; M.R. Hamid; M. Himdi; H.B.A. Majid; N.A. Samsuri 25. Reconfigurable Dual Band Antenna Using HIS-EBG Unit Cells for Changing Pattern and Frequency. 2018;76:123-132 in Progress in Electromagnetic Research. [CrossRef]

30. A. Zeng, Q. Ma, R. Zeng, and L. Han. The development of a wideband slot antenna that can change its frequency and radiation pattern. 2018 Int. J. Antennas Propag. [CrossRef]

31. Antenna Theory and Design, by W.L. Stutzman and G.A. Thiele, was published by John Wiley & Sons in 2013 (pages 27).

32. Far-field analysis of the RF front-end performance of reconfigurable antennas using RF switches. Yeom, I.; Choi, J.; Kwoun, S.s.; Lee, B.; Jung, C. Antennas Propagation International 2014;2014(385730). [CrossRef]